

Tumors as Elasto-Viscoplastic Growing Bodies

D. Ambrosi, L. Preziosi

Dipartimento di Matematica, Politecnico di Torino

Corso Duca degli Abruzzi 24, I-10129, Torino, Italy,

davide.ambrosi@polito.it - luigi.preziosi@polito.it

June 17, 2007

Abstract

Tumor cells usually duplicate in a environment formed by other host cells, a deformable extra-cellular matrix and of extra-cellular liquid. Cells duplicate, reorganize and deform while binding each other through adhesion molecules that have a limited strength that can be measured. These observations motivate the multiphase mechanical model illustrated in the present work.

The extracellular matrix is treated as an elastic compressible material, while, in order to define the relationship between stress and strain for the cellular constituents, the deformation gradient is decomposed in a multiplicative way distinguishing the contribution due to growth, to plastic rearrangement of the cells and to elastic deformation. On the basis of experimental results at a cellular level, it is proposed that a continuum level there exists a yield condition separating the elastic and viscoplastic regimes. Previously proposed models are obtained as limit cases, e.g. fluid-like models are obtained in the limit of fast cell re-organization and negligible yield stress. A test case is studied in detail showing how tumor growth can be influenced by stress, how and where it can generate plastic reorganization of the cells, how it can lead to capsule formation and compression of the surrounding tissue.

Introduction

Most research on solid tumors historically focuses on determining the interplay between the biochemical factors that promote or inhibit growth and angiogenesis. Mechanical effects have been neglected for a long time, until recent experiments have shown that they play a non-negligible role. As an example, Helmlinger *et al.* measured the diameter of growing cellular spheroids in gels of different rigidity and demonstrate that the tumor size depends on the normal load exerted by the surrounding gel on the multicellular spheroid [24].

The modelling literature devoted to such mechanisms has appeared just in recent years. In absence of extensive experimental data, several approaches have been proposed, based on very different assumptions, the main differences being summarized below.

1. The mechanical stress-strain constitutive equation. Most models use fluid-like constitutive equations [3, 9, 10, 12, 13, 16, 17, 19, 20, 21], others adopt a linear elastic one [4, 5, 6, 29, 40]. Tumors are therefore considered as an aggregate of soft balloons that roll on each other in a continuum limit (visco-elastic fluid) or take inspiration from biological soft tissues models (nonlinear elasticity). These differences are somehow hidden in the equations when spherical symmetry and incompressibility are assumed, so that geometry dominates mechanics, but they become most evident when a real three-dimensional modelling is faced.
2. Restricting to the papers describing the tumor as a solid mass, the papers mentioned above develop under the observation that tumors are a mixture of several biological components, while others simplify the description to one-component theory describing more precisely the relation between elastic stress and growth [1, 2].

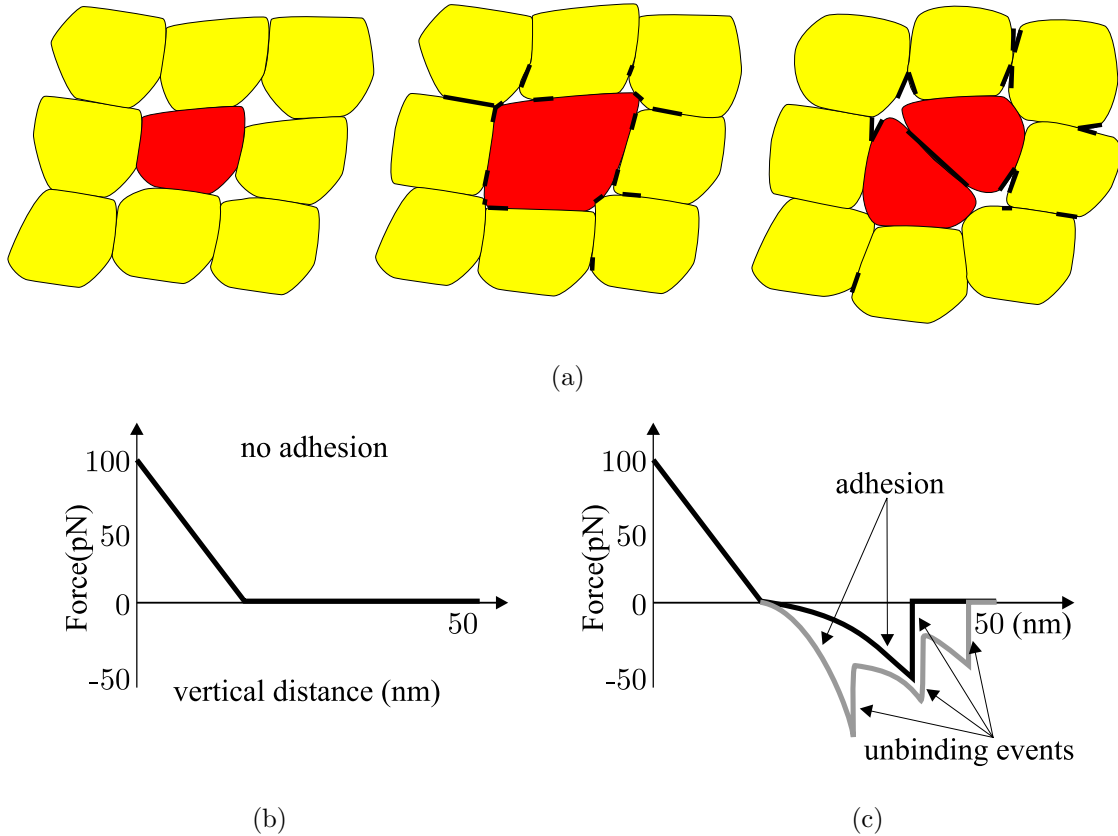


Figure 1: (a) Sketch of pseudo-plastic behavior during tumor growth. Thicker lines indicate where there is a reorganization of adhesion bonds, e.g., broken or newly formed. (b) and (c) refer to classical output from adhesive force measurement (redrawn from [8, 35, 44]). Adhesiveness acts as an elastic nonlinear spring. However, when the force is too strong, then bonds break, giving rise to single or multiple unbinding events.

3. The mathematical modelling of growth poses several questions about the stress–growth relationships and the possible inclusion of residual stress in the formulation; some authors neglect them [17], while others do not [1].

The aim of this paper is to critically collect in a unifying mathematical framework the many partial contributions sketched in the list above. We illustrate the mathematical properties of the equations that model a growing tumor as a mixture of three components (cell, matrix, liquid). Tumor remodelling evolves according to the theory proposed for biological tissues in [26, 27, 39] and specifically applied to tumor growth in [1, 2], which is based on a multiplicative decomposition of the tensor gradient of deformation: growth and elastic deformation. The reader is referred to [33] for a unified treatment. According to such a methodology, Ambrosi and Mollica [2] use a purely elastic one–component model to evaluate residual stress formation in a growing multicellular spheroid. Although the qualitative behavior of the solution is the expected one, the values they find by numerical simulations are very large and this suggests that in their fully elastic model some mechanism of stress relaxation is neglected.

Stress relaxation at a macroscopic level is introduced in the present paper on the basis of cellular arguments. It is known that cells adhere each other via cadherin junctions and to the extra-cellular matrix via integrin junctions. However, as shown in Fig. 1, these bonds have a limited strength as measured, for instance, by Baumgardner et al. [8], Canetta et al. [14], Panorchan et al. [35], and Sun *et al.* [44]. In typical experiments to test the adhesive strength of a cell, a microsphere

adheres to the tip of an atomic force microscopy cantilever. After putting the microsphere in contact with the cell, the cantilever is pulled away at a constant speed.

Baumgardner et al. [8] properly functionalized the bead to achieve a strong attachment with the vascular endothelial cadherins secreted by transfected Chinese hamster ovary cells and allowed a resting period on the cell surface of the order of one second. When the cantilever was pulled away at a constant speed (in the range $0.2\text{--}4\ \mu\text{m}/\text{sec}$) adhesion caused the deflection of the cantilever. From that they obtained a measurement of the stretching force characterised by jumps indicating the rupture of adhesive bonds, as shown in Fig. 1c. Actually, since a sphere binds to many receptors, they often observed multiple unbinding events occurring at different times, as shown by the grey curve in Fig. 1c. From such jumps they concluded that the adhesive strength of a single bond was in the range of $35\text{--}55\ \text{pN}$.

A similar experiment was repeated by Sun et al. [44] without functionalising the bead and allowing a longer resting period on the cell surface, ranging from 2 to 30 seconds. Again, pulling away the cantilever at a constant speed in the range $3\text{--}5\ \mu\text{m}/\text{sec}$ caused the rupture of some adhesive bonds. In this case, in addition to Chinese hamster ovary cells, endothelial cells and human brain tumor cells were used. All cell types gave an adhesive strength of a single bond slightly below $30\ \text{pN}$. Coating the bead with poly-L-lysine or collagen did not lead to significant changes in the measurement.

Instead, Panorchan et al. [35] attached to the cantilever a cadherin-expressing cell that was then put in contact with a similar cell attached to the substratum. The time of contact was kept short in order to have the formation of a very limited number of adhesion bonds. The rupture force was then found to increase with the loading rate and that it was much smaller when N-cadherin bonds were involved (up to $40\ \text{pN}$) than when E-cadherin bonds were involved (up to $73\ \text{pN}$ for a loading rate of $1000\ \text{pN}/\text{s}$ and $157\ \text{pN}$ for a loading rate of $10000\ \text{pN}/\text{s}$).

On the other hand, interfering with the adhesion mechanism gives rise to big differences. Baumgardner et al. [8] achieved that by the addition of an antibody of the vascular endothelial cadherin external domain and obtained a behavior of the measured force as that shown in Fig. 1b, leading to the conclusion that there is no adhesion between the bead and the cell. A similar method was used in [35] to verify the specificity of cadherin-mediated interaction.

Sun et al. [44] used latrunculin A to disrupt the actin cytoskeleton in a concentration dependent way. In these cases the adhesion decreased down to $15\ \text{pN}$. A comparable result was obtained treating the cells with hyaluronidase. A similar ratio was also obtained by Canetta et al. [14] who measured the adhesion force of intercellular adhesion molecules-1 (ICAM-1) when they were properly linked to the actin cytoskeleton and when it was not, due to the expression of a mutant form of ICAM-1 without its cytoplasmic domain, so that they could not be anchored properly to the actin cytoskeleton.

This phenomenological cellular (molecular) description can then be schematised at the tissue level as follows: if an ensemble of cells is subject to a sufficiently high tension or shear, some bonds break and some others form. This kind of phenomenology suggests the existence of a yield stress and therefore the use of a plastic deformation formalism in the continuum mechanics modelling of solid tumors. In particular, the mechanism of cell attachment–detachment can be relevant during growth under an external load, when duplicating cells displace their neighbors, as sketched in Fig. 1a.

The paper then develops as follows. In the first section a general multiphase framework is developed considering the tumor (or the tissue) as made of cells, extracellular matrix and extracellular liquid. However, having in mind that we want to describe the tumor as a solid material for moderate stresses, then in the same section we introduce the basic concepts of multiple natural configurations. Section 2 then describe a constitutive model able to include the yield phenomena mentioned above. Limit cases are also worked out to understand the link between previously applied models and the one presented here. Finally, in Section 3 a one-dimensional problem is studied in detail showing how tumor growth can be influenced by stress, how and where it can generate plastic reorganization of the cells, how it can lead to capsule formation and compression of the surrounding tissue.

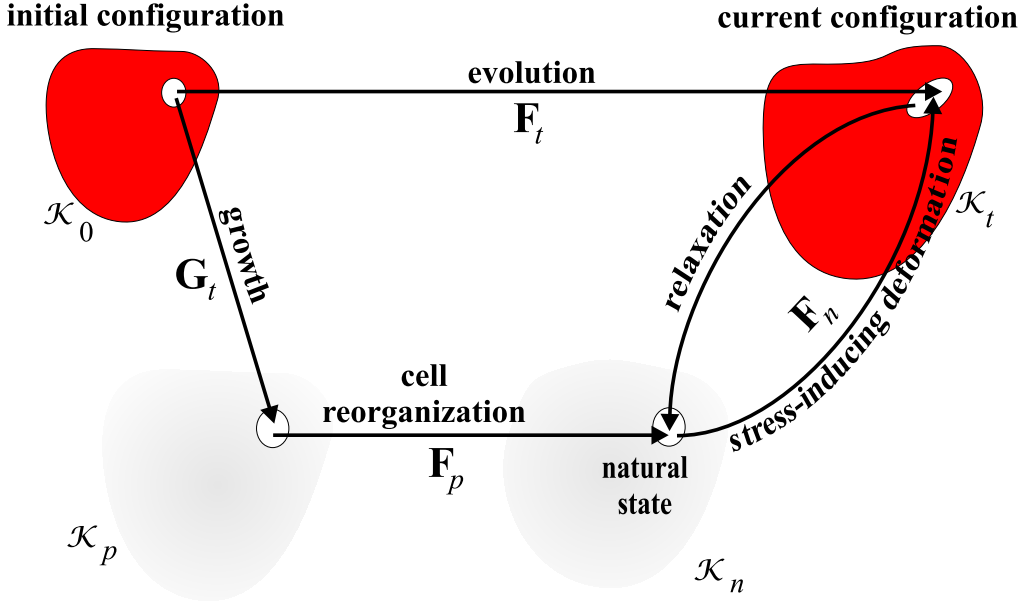


Figure 2: Multiple natural configuration.

1 The Multiphase Model

1.1 Kinematics

A tumor is made of many constituents, including tumor cells, extracellular matrix (ECM) and extracellular liquid. Nutrients and chemical factors diffuse in the liquid and are absorbed/produced by the cells; they play a relevant energetic role in growth but not in mass and force balance and are neglected in the present work. Cells live, move and duplicate in the extracellular matrix. In the present work, we assume that the ECM is neither degraded nor produced by the cells. As usual in multiphase theory, we associate every component with its own deformation gradient defined in every point of the mixture.

In the deformation gradient \mathbf{F}_t of the tumor component we distinguish the contributions of pure growth, plastic deformation and elastic deformation by a multiplicative decomposition. This splitting is suggested also by the observation that growth occurs on a much longer time scale (hours up to days) than deformation.

The deformation gradient \mathbf{F}_t is a mapping from a tangent space onto another tangent space, and it indicates how the body is deforming locally in going from the initial (reference) configuration \mathcal{K}_0 to the current configuration \mathcal{K}_t . A point of the body is imagined to relieve its state of stress while relaxing the requirement of its integrity. It then relaxes to a stress-free configuration. The atlas of these pointwise configurations forms what we define natural configuration with respect to \mathcal{K}_t and denote by \mathcal{K}_n . Of course, this natural configuration depends on time. Referring to Figure 2, we identify this deformation without growth with the tensor \mathbf{F}_n , which then describes how the body is deforming locally while going from the natural configuration \mathcal{K}_n to \mathcal{K}_t .

With respect to the initial configuration \mathcal{K}_0 the particle in the configuration \mathcal{K}_n has possibly undergone both growth and plastic deformation due to unbinding and rebinding events. One can then again consider the map from \mathcal{K}_0 to \mathcal{K}_n as composed of two parts: the first one related to growth/death processes (therefore to mass variations in the volume element), the second one due to internal re-organization, which implies re-arranging of the adhesion links among the cells, without change of mass in the volume element. Denoting by \mathcal{K}_p the “grown configuration”, i.e., the intermediate configuration of the body between \mathcal{K}_0 and \mathcal{K}_n , we will assume that for any given

point the volume ratio in \mathcal{K}_p is the same as in the natural configuration \mathcal{K}_n and in the original reference configuration \mathcal{K}_0 , i.e., $\phi_p = \phi_t(t=0) = \phi_n$.

According to the three-steps process outlined above, the deformation gradient is splitted as

$$\mathbf{F}_t = \mathbf{F}_n \mathbf{F}_p \mathbf{G}_t. \quad (1.1)$$

or

$$\mathbf{F}_n = \mathbf{F}_t \mathbf{G}_t^{-1} \mathbf{F}_p^{-1}. \quad (1.2)$$

According to Equation (1.2) the part of the deformation gradient leading to recoverable energy \mathbf{F}_n is obtained eliminating from the observable deformation gradient \mathbf{F}_t the contributions related to the dissipative processes due to growth and plasticity.

Denoting by dV , dV_p , dV_n , and dv the volume elements in the initial, grown, natural and current configuration, respectively, the related masses are then $dM = \rho\phi_n dV$, $dm = \rho\phi_p dV_p = \rho\phi_n dV_n = \rho\phi_t dv$ where it can be noticed that mass is preserved between \mathcal{K}_p and \mathcal{K}_t , through \mathcal{K}_n . One then has that

$$\begin{aligned} J_t = \det \mathbf{F}_t &= \frac{dv}{dV} = \frac{\phi_n}{\phi_t} \frac{dm}{dM}, \\ J_g = \det \mathbf{G}_t &= \frac{dV_p}{dV} = \frac{\phi_n}{\phi_p} \frac{dm}{dM} = \frac{dm}{dM}, \\ J_p = \det \mathbf{F}_p &= \frac{dV_n}{dV_p} = \frac{\phi_p}{\phi_n} = 1, \\ J_n = \det \mathbf{F}_n &= \frac{dv}{dV_n} = \frac{\phi_n}{\phi_t}, \end{aligned} \quad (1.3)$$

and, of course,

$$J_t = J_g J_p J_n = J_g J_n. \quad (1.4)$$

Net growth corresponds to $J_g > 1$ and net death to $J_g < 1$. Of course, J_g never vanishes, otherwise \mathbf{F}_t would be singular.

It will be useful to differentiate Equation (1.3d) to get

$$\frac{d}{dt} \log(\phi_t J_n) = 0, \quad (1.5)$$

where the time derivative is a convective derivative computed using the velocity of the transported component. Similarly, differentiating $J_t = J_g J_n$, one has

$$\frac{1}{J_t} \frac{dJ_t}{dt} = \frac{1}{J_g} \frac{dJ_g}{dt} + \frac{1}{J_n} \frac{dJ_n}{dt}, \quad (1.6)$$

or, using (1.5),

$$\frac{1}{J_g} \frac{dJ_g}{dt} = \frac{1}{\phi_t} \left(\frac{d\phi_t}{dt} + \frac{\phi_t}{J_t} \frac{dJ_t}{dt} \right). \quad (1.7)$$

The mass balance equations for the constituents can be written as

$$\begin{aligned} \frac{\partial \phi_0}{\partial t} + \nabla \cdot (\phi_0 \mathbf{v}_0) &= 0, \\ \frac{\partial \phi_t}{\partial t} + \nabla \cdot (\phi_t \mathbf{v}_t) &= \Gamma_t, \\ \frac{\partial \phi_\ell}{\partial t} + \nabla \cdot (\phi_\ell \mathbf{v}_\ell) &= -\Gamma_t. \end{aligned} \quad (1.8)$$

According to the terms on the r.h.s. the tumor exchanges mass with the extracellular liquid only.

Using Equations (1.7) and (1.8) we find

$$\frac{\dot{J}_g}{J_g} = \frac{1}{\phi_t} \left(\Gamma_t - \phi_t \nabla \cdot \mathbf{v}_t + \frac{\phi_t \dot{J}_t}{J_t} \right) = \frac{\Gamma_t}{\phi_t} + \frac{1}{J_t} \left(\dot{J}_t - J_t \nabla \cdot \mathbf{v}_t \right) = \frac{\Gamma_t}{\phi_t}. \quad (1.9)$$

where upper dot denotes time differentiation following the tumor cells.

In the following we will assume spherical growth: $\mathbf{G}_t = g\mathbf{I}$. In this case $J_g = g^3$ and (1.9) rewrites as

$$\dot{g} = \frac{\Gamma_t}{\phi_t} \frac{g}{3}. \quad (1.10)$$

Given Γ_t , the equation above describes how \mathbf{G}_t evolves as a function of ϕ_t and all the other variables Γ_t depends upon, and therefore how \mathcal{K}_p evolves.

It is convenient to re-write the equations in Lagrangean form using a frame of reference fixed on the extra-cellular matrix, which has no mass sources. One then has [46]

$$\begin{aligned} \frac{\partial_0}{\partial t}(\phi_0 J_0) &= 0, \\ \frac{\partial_0}{\partial t}(\phi_t J_0) + \text{Div}_0[\phi_t J_0 \mathbf{F}_0^{-1}(\mathbf{v}_t - \mathbf{v}_0)] &= \Gamma_t J_0, \\ \frac{\partial_0}{\partial t}(\phi_\ell J_0) + \text{Div}_0[\phi_\ell J_0 \mathbf{F}_0^{-1}(\mathbf{v}_\ell - \mathbf{v}_0)] &= -\Gamma_t J_0, \end{aligned} \quad (1.11)$$

where $\partial_0/\partial t$ and Div_0 are differential operators in a frame of reference fixed on the ECM.

Note that if saturation is assumed, then $\phi_t + \phi_\ell + \phi_0 = 1$. Summing then the mass balance equations, thanks to the fact that the mixture is closed one has

$$\nabla \cdot \mathbf{v}_c = 0, \quad (1.12)$$

or in Lagrangean form

$$\frac{\partial_0 J_0}{\partial t} + \text{Div}_0[J_0 \mathbf{F}_0^{-1}(\mathbf{v}_c - \mathbf{v}_0)] = 0, \quad (1.13)$$

where $\mathbf{v}_c = \phi_t \mathbf{v}_t + \phi_\ell \mathbf{v}_\ell + \phi_0 \mathbf{v}_0$ is called composite velocity.

1.2 Dynamics

The momentum equation for the constituents can be written neglecting inertia and assuming, as usual when dealing with slow flow in porous materials, that the main contribution to the interaction force between the constituents is proportional to the relative velocity between the constituents [3]. One then has

$$\begin{aligned} 0 &= -\phi_0 \nabla P + \nabla \cdot \mathbf{T}_0 - \mathbf{M}_{t0}(\mathbf{v}_0 - \mathbf{v}_t), \\ 0 &= -\phi_t \nabla P + \nabla \cdot \mathbf{T}_t - \mathbf{M}_{\ell t}(\mathbf{v}_t - \mathbf{v}_\ell) - \mathbf{M}_{t0}(\mathbf{v}_t - \mathbf{v}_0), \\ 0 &= -\phi_\ell \nabla P - \mathbf{M}_{\ell t}(\mathbf{v}_\ell - \mathbf{v}_t). \end{aligned} \quad (1.14)$$

where the extracellular liquid is treated as an inviscid fluid in light of the usual assumptions used to get Darcy's law from mixture theory. Here we also assume that the interaction force between liquid and ECM is negligible compared to the interaction force exerted by the cells on the ECM or the drag of the cells by the liquid. However, its inclusion is technical leading to a model made more complex by the presence of extra terms. General constitutive models for cell-ECM interactions are studied in [38] that focus on adhesion mechanisms between cells and ECM.

Introducing the permeability tensor $\mathbf{K} = \phi_\ell^2 \mathbf{M}_{\ell t}^{-1}$ and $\mathbf{K}_0 = \phi_0^2 \mathbf{M}_{0t}^{-1}$, and writing the momentum equation of the mixture, one has

$$\begin{aligned} \mathbf{v}_0 - \mathbf{v}_t &= \frac{\mathbf{K}_0}{\phi_0^2} (-\phi_0 \nabla P + \nabla \cdot \mathbf{T}_0), \\ \mathbf{v}_\ell - \mathbf{v}_t &= -\frac{\mathbf{K}}{\phi_\ell} \nabla P, \\ 0 &= -\nabla P + \nabla \cdot (\mathbf{T}_0 + \mathbf{T}_t), \end{aligned} \quad (1.15)$$

which can be written in the Lagrangean framework defined by the ECM.

The stress tensors in the equations above account for partial stress, i.e. the stress of each component in the mixture, which depend on the respective volume fraction at least linearly, as remarked for instance in Truesdell [23].

2 Stress Constitutive Model

This section is devoted to stating the constitutive assumptions for the components of the mixture. We assume that the ECM behaves as a compressible elastic body, satisfying

$$\mathbf{T}_0 = \phi_0 \hat{\mathbf{T}}_0(\mathbf{B}_0), \quad (2.1)$$

where $\mathbf{B}_0 = \mathbf{F}_0 \mathbf{F}_0^T$.

On the other hand, inclusion of visco-plastic effects in the mechanics of cell aggregates goes along the following intuitive descriptions:

1. when and where the cell populations is subject to a moderate amount of stress, then the body behaves elastically;
2. when and where the stress overcomes a threshold yield stress then the body undergoes visco-plastic deformations.

Defining

$$\mathbf{D}_p = \text{sym}(\dot{\mathbf{F}}_p \mathbf{F}_p^{-1}), \quad (2.2)$$

from standard tensor calculus one has that

$$\dot{J}_p = J_p \text{tr} \mathbf{D}_p, \quad (2.3)$$

and therefore because of (1.3)₃

$$\text{tr} \mathbf{D}_p = 0. \quad (2.4)$$

Regarding the definition of yield stress, referring to Fig. 1, if the resistance of a single bond can be considered nearly constant, the threshold level identifying the appearance of plastic deformations is proportional to the area of the cell membranes in contact, that depends on the number of cells per unit volume. In absence of additional experimental evidences, we assume a proportionality rule between yield stress and tumor cells volume fraction though in reality the relation might be more complex. In fact, one should distinguish situations in which the volume ratio is so small that cells hardly touch and situation in which cells are closely packed. In the former case, the transfer of stress is very hard and yield stress is very low. In the second case, borrowing ideas from the dynamics of colloidal particles and flocculated suspensions, it seems that the yield stress increases with the second or the third power of the volume ratio [11, 43].

On this basis, the following elastic-type constitutive equation can be suggested in the elastic regime

$$\mathbf{T}_t = \phi_t \hat{\mathbf{T}}_t(\mathbf{B}_n), \quad \text{if } f(\mathbf{T}_t) \leq \phi_t \tau, \quad (2.5)$$

where $\mathbf{B}_n = \mathbf{F}_n \mathbf{F}_n^T$.

In general, the function $f(\mathbf{T}_t)$ is a general frame invariant measure of the stress, vanishing for $\mathbf{T}_t = 0$, homogeneous of degree one, i.e.

$$f(\alpha \mathbf{T}_t) = |\alpha| f(\mathbf{T}_t), \quad (2.6)$$

to be specified in the following.

Following [7, 42], above the yield stress the tension in excess originates from cell unbinding at the microscopic scale and then cell rearrangement at the macroscopic scale. Such a pictorial description is put into formal terms by the following constitutive equation

$$\left[1 - \frac{\phi_t \tau}{f(\mathbf{T}_t - \frac{1}{3}(\text{tr} \mathbf{T}_t) \mathbf{I})} \right] \left(\mathbf{T}_t - \frac{1}{3}(\text{tr} \mathbf{T}_t) \mathbf{I} \right) = 2\eta_p \phi_t \mathbf{D}_p, \quad \text{if } f\left(\mathbf{T}_t - \frac{1}{3}(\text{tr} \mathbf{T}_t) \mathbf{I}\right) > \phi_t \tau. \quad (2.7)$$

Notice that the left hand side of equation (2.7) is traceless and therefore the incompressibility constraint (2.4) always applies. In addition, we remark that the factor in square brackets on the left hand side is always positive, otherwise the mathematical problem would be ill-posed.

We observe that using the more general form

$$\left[1 - \frac{\phi_t \tau}{f(\mathbf{T}_t - \alpha \mathbf{I})}\right] (\mathbf{T}_t - \alpha \mathbf{I}) = -\beta \mathbf{I} + 2\eta_p \phi_t \mathbf{D}_p, \quad \text{if } f(\mathbf{T}_t - \alpha \mathbf{I}) > \phi_t \tau, \quad (2.8)$$

with generic α and β leads again to (2.7). In fact, applying the trace operator and recalling Eq. (2.4), one has that $\alpha = \frac{1}{3}(\text{tr} \mathbf{T}_t) \mathbf{I}$ and $\beta = 0$.

It is instructive to look closely at what happens at criticality, i.e. when

$$f\left(\mathbf{T}_t - \frac{1}{3}(\text{tr} \mathbf{T}_t) \mathbf{I}\right) = \phi_t \tau. \quad (2.9)$$

In this case, Eq. (2.7) implies that $\mathbf{D}_p = \mathbf{0}$ (and therefore $\dot{\mathbf{F}}_p = \mathbf{0}$) which means that no contribution to the evolution of the natural configuration is due to plastic deformations, while the system stays on (or inside) the yield surface. A contribution is instead generated when the system crosses the yield surface.

The relationship (2.8) can be rewritten in a more usual form applying the function f to both sides of (2.7), giving the relation

$$f\left(\left[1 - \frac{\phi_t \tau}{f\left(\mathbf{T}_t - \frac{1}{3}(\text{tr} \mathbf{T}_t) \mathbf{I}\right)}\right] \left(\mathbf{T}_t - \frac{1}{3}(\text{tr} \mathbf{T}_t) \mathbf{I}\right)\right) = f(2\eta_p \phi_t \mathbf{D}_p), \quad (2.10)$$

or, thanks to the homogeneity of f expressed in (2.6),

$$2\eta_p \phi_t f(\mathbf{D}_p) = \left[1 - \frac{\phi_t \tau}{f\left(\mathbf{T}_t - \frac{1}{3}(\text{tr} \mathbf{T}_t) \mathbf{I}\right)}\right] f\left(\mathbf{T}_t - \frac{1}{3}(\text{tr} \mathbf{T}_t) \mathbf{I}\right) = f\left(\mathbf{T}_t - \frac{1}{3}(\text{tr} \mathbf{T}_t) \mathbf{I}\right) - \phi_t \tau. \quad (2.11)$$

This relation can be substituted back in (2.7) to give

$$\left[1 - \frac{\phi_t \tau}{\phi_t \tau + 2\eta_p \phi_t f(\mathbf{D}_p)}\right] \left(\mathbf{T}_t - \frac{1}{3}(\text{tr} \mathbf{T}_t) \mathbf{I}\right) = 2\eta_p \phi_t \mathbf{D}_p, \quad \text{if } f\left(\mathbf{T}_t - \frac{1}{3}(\text{tr} \mathbf{T}_t) \mathbf{I}\right) > \phi_t \tau, \quad (2.12)$$

or

$$\mathbf{T}_t = \frac{1}{3}(\text{tr} \mathbf{T}_t) \mathbf{I} + \left[2\eta_p + \frac{\tau}{f(\mathbf{D}_p)}\right] \phi_t \mathbf{D}_p, \quad \text{if } f\left(\mathbf{T}_t - \frac{1}{3}(\text{tr} \mathbf{T}_t) \mathbf{I}\right) > \phi_t \tau, \quad (2.13)$$

which more closely resembles the usual form of constitutive equation of Bingham fluids used in the literature. However, in the following sections we refer to the form (2.7) because it directly provides the evolution of \mathbf{F}_p .

There are several possible choices of the function f . The three-dimensional generalization of Bingham constitutive law proposed by Hohenemser and Prager [25] reads

$$f(\mathbf{P}) \equiv f_1(\mathbf{P}') = \sqrt{\frac{\mathbf{P}' : \mathbf{P}'}{2}}, \quad (2.14)$$

where $\mathbf{P}' = \mathbf{P} - \frac{\text{tr} \mathbf{P}}{3} \mathbf{I}$. Basov and Shelukhin [7] instead suggest to base the measure on

$$\mathbf{p}(\mathbf{n}) = \mathbf{P} \mathbf{n} - (\mathbf{n} \cdot \mathbf{P} \mathbf{n}) \mathbf{n}, \quad (2.15)$$

that represents the tangential stress vector relative to the surface identified by the normal \mathbf{n} . Therefore the quantity

$$f(\mathbf{P}) \equiv f_2(\mathbf{P}) = \max_{|\mathbf{n}|=1} |\mathbf{p}(\mathbf{n})|, \quad (2.16)$$

is the maximum shear stress magnitude occurring in the plane identified by the eigenvector corresponding to the maximum of $|\mathbf{p}(\mathbf{n})|$. It can be proved (see, for instance, [31]) that f_2 is given by half of the difference between the maximum and the minimum eigenvalue of \mathbf{P} .

Besov and Shelukin [7] suggest the following form:

$$f(\mathbf{P}) = f_3(\mathbf{P}) = \sqrt{f_2^2(\mathbf{P}) + (\text{tr}\mathbf{P})^2}.$$

However, in our case the argument of f is traceless and therefore $f_2 = f_3$.

In conclusion, assuming that the tumor component obeys to a neo-Hookean nonlinear elastic law, the following constitutive equation can be suggested

$$\mathbf{T}_t = \phi_t(-\Sigma_t \mathbf{I} + \mu_t \mathbf{B}_n) = \phi_t \left(-\Sigma_t \mathbf{I} + \frac{\mu_t}{g^2} \mathbf{F}_t \mathbf{C}_p^{-1} \mathbf{F}_t^T \right), \quad (2.17)$$

where $\Sigma_t = \Sigma_t(\phi_t/\phi_n)$, with $\Sigma_t(1) = \mu_t$, and $\mathbf{C}_p = \mathbf{F}_p^T \mathbf{F}_p$, and \mathbf{F}_p evolves according to

$$\dot{\mathbf{F}}_p = \begin{cases} \mathbf{0}, & \text{if } f(\mathbf{B}_n - \frac{1}{3}(\text{tr}\mathbf{B}_n)\mathbf{I}) \leq \frac{\tau}{\mu_t}; \\ \frac{\mu_t}{2\eta_p} \left[1 - \frac{\tau}{\mu_t f(\mathbf{B}_n - \frac{1}{3}(\text{tr}\mathbf{B}_n)\mathbf{I})} \right] \left(\mathbf{B}_n - \frac{1}{3}(\text{tr}\mathbf{B}_n)\mathbf{I} \right) \mathbf{F}_p, & \text{if } f(\mathbf{B}_n - \frac{1}{3}(\text{tr}\mathbf{B}_n)\mathbf{I}) > \frac{\tau}{\mu_t}. \end{cases} \quad (2.18)$$

or, in a more compact form,

$$\dot{\mathbf{F}}_p = \frac{\mu_t}{2\eta_p} \left[1 - \frac{\tau}{\mu_t f(\mathbf{B}_n - \frac{1}{3}(\text{tr}\mathbf{B}_n)\mathbf{I})} \right]_+ \left(\mathbf{B}_n - \frac{1}{3}(\text{tr}\mathbf{B}_n)\mathbf{I} \right) \mathbf{F}_p, \quad (2.19)$$

where $[\cdot]_+$ stands for the positive part of the argument.

It is of course possible to generalize the constitutive model above to include possible shear-thinning effects by allowing a dependence of η_p from \mathbf{D}_p , e.g.,

$$\eta_p = m |\mathbb{I}_{D_p}|^{(n-1)/2} \quad (2.20)$$

where the coefficient n is related to the slope of the shear stress behavior versus the shear rate. In this way one obtains a constitutive equation similar to Herschel–Buckley model.

In order to explain phenomenologically Eq. (2.19), consider the case of absence of growth. If the body undergoes a deformation corresponding to a stress below the yield stress, then \mathbf{F}_p does not change, i.e., the natural configuration does not evolve (we are in the case of absence of growth, too) and all the energy is elastically stored and can be recovered. If the deformation corresponds to a value above the yield stress, then the natural configuration changes to release the stress in excess to a sustainable value, until the yield surface defined by f is reached again. The ratio η_p/μ_t gives an indication of the characteristic time needed to reach the yield surface again.

2.1 Limit Cases

In this section we examine how our model compares with previously proposed ones. In fact, some attempts were done in the literature to describe growing tumors alternatively as elastic solids [4, 5, 6, 29] or fluids [3, 9, 10, 12, 13, 16, 17, 19, 20, 21], including stress relaxation while avoiding the split of the deformation gradient into growth and deformation. Usual assumptions in the former case are incompressibility of the cell component and a linear elastic behavior. Plastic or visco-plastic deformations are neglected.

More specifically, Jones and coworkers [29] and Araujo and McElwain [4, 5, 6] propose

$$\mathbf{T}'_t = \frac{2}{3} E \left(\mathbf{E}_t - \frac{1}{3}(\text{tr}\mathbf{E}_t)\mathbf{I} \right), \quad (2.21)$$

where $\mathbf{T}'_t = \mathbf{T}_t - \frac{1}{3}(\text{tr}\mathbf{T}_t)\mathbf{I}$ and \mathbf{E}_t is the infinitesimal strain tensor. The same Authors propose to rewrite the constitutive equation in terms of the rate of stress as

$$\dot{\mathbf{T}}'_t + \mathbf{W}_t \mathbf{T}'_t - \mathbf{T}'_t \mathbf{W}_t = \frac{2}{3}E \left(\mathbf{D}_t - \frac{1}{3}(\nabla \cdot \mathbf{v}_t)\mathbf{I} \right) \quad (2.22)$$

where $\mathbf{W}_t = (\nabla \mathbf{v}_t - \nabla \mathbf{v}_t^T)/2$ is the vorticity tensor. The particular time derivative appearing at the left hand side of equation (2.22) yields a frame indifferent relationship, provided that \mathbf{T}_t is frame invariant. Unfortunately, this is no case for \mathbf{T}_t in (2.21) and for \mathbf{E}_t and therefore its use is inappropriate in the linear theory (see, for instance, [31], page 403).

In order to compare Equations (2.21) and (2.22) with the model proposed in the present paper, a linear version has to be obtained in the small strain limit.

The small deformation assumption applies depending on the value of the yield stress: it has to be small enough so that the condition $|\mathbf{B}_n \cdot \mathbf{I} - 3| \ll 1$ is always satisfied during the motion. Note that for tensions larger than 0.1 kPA, cell adhesion bonds break up [8], thus giving an indication of the order of magnitude of the yield stress. For small elastic strain one can use linear elasticity below the yield surface. For larger stress, the natural configuration evolves. If the relaxation of stresses is much faster than growth, as it should be, then the deformation with respect to the natural configuration due to growth are kept small during the evolution.

Still with the aim of comparing our result with previous works we impose the incompressibility constraint to tumor matter ($J_n = 1$), the spherical part of the stress tensor is replaced by a Lagrangian multiplier P_t , so that elastic constitutive equation rewrites

$$\mathbf{T}'_t = \mu_t \phi_n \left(\mathbf{B}_n - \frac{1}{3}(\text{tr}\mathbf{B}_n)\mathbf{I} \right), \quad (2.23)$$

where $\mathbf{T}_t = -P_t \mathbf{I} + \mathbf{T}'_t$. Deriving (2.23), one has

$$\dot{\mathbf{T}}'_t = \mu_t \phi_n \left(\dot{\mathbf{B}}_n - \frac{1}{3}(\text{tr}\dot{\mathbf{B}}_n)\mathbf{I} \right), \quad (2.24)$$

where

$$\dot{\mathbf{B}}_n = \mathbf{L}_n \mathbf{B}_n + \mathbf{B}_n \mathbf{L}_n^T, \quad (2.25)$$

with

$$\mathbf{L}_n = \dot{\mathbf{F}}_n \mathbf{F}_n^{-1}. \quad (2.26)$$

On the other hand, deriving $\mathbf{F}_t = g \mathbf{F}_n \mathbf{F}_p$ in time, one has

$$\begin{aligned} \dot{\mathbf{F}}_t &= \dot{g} \mathbf{F}_n \mathbf{F}_p + g \dot{\mathbf{F}}_n \mathbf{F}_p + g \mathbf{F}_n \dot{\mathbf{F}}_p = \dot{g} g^{-1} \mathbf{F}_t + g \mathbf{L}_n \mathbf{F}_n \mathbf{F}_p + g \mathbf{F}_n \mathbf{D}_p \mathbf{F}_p \\ &= (\dot{g} g^{-1} \mathbf{I} + \mathbf{L}_n + \mathbf{F}_n \mathbf{D}_p \mathbf{F}_n^{-1}) \mathbf{F}_t. \end{aligned} \quad (2.27)$$

Hence, defining as usual, $\mathbf{L}_t = \dot{\mathbf{F}}_t \mathbf{F}_t^{-1}$ one can write

$$\mathbf{L}_n = \mathbf{L}_t - \dot{g} g^{-1} \mathbf{I} - \mathbf{F}_n \mathbf{D}_p \mathbf{F}_n^{-1}, \quad (2.28)$$

which can be substituted back in (2.25) to give

$$\dot{\mathbf{B}}_n = \mathbf{L}_t \mathbf{B}_n + \mathbf{B}_n \mathbf{L}_t^T - 2\dot{g} g^{-1} \mathbf{I} - 2\mathbf{F}_n \mathbf{D}_p \mathbf{F}_n^T. \quad (2.29)$$

In the limit of small deformations, (2.29) reduces to leading order to

$$\dot{\mathbf{B}}_n \approx 2(\mathbf{D}_t - \dot{g} g^{-1} \mathbf{I} - \mathbf{D}_p). \quad (2.30)$$

Recalling that $\text{tr}\mathbf{D}_p = 0$, one then has that

$$\dot{\mathbf{B}}_n - \frac{1}{3}(\text{tr}\dot{\mathbf{B}}_n)\mathbf{I} \approx 2 \left(\mathbf{D}_t - \mathbf{D}_p - \frac{1}{3}(\text{tr}\mathbf{D}_t)\mathbf{I} \right), \quad (2.31)$$

and therefore from (2.24)

$$\dot{\mathbf{T}}'_t = 2\mu_t\phi_n \left(\mathbf{D}_t - \mathbf{D}_p - \frac{1}{3}(\nabla \cdot \mathbf{v}_t)\mathbf{I} \right), \quad (2.32)$$

or, recalling (2.7),

$$\dot{\mathbf{T}}'_t + \frac{\mu_t}{\eta_p} \left[1 - \frac{\phi_n\tau}{f(\mathbf{T}'_t)} \right]_+ \mathbf{T}'_t = 2\mu_t\phi_n \left(\mathbf{D}_t - \frac{1}{3}(\nabla \cdot \mathbf{v}_t)\mathbf{I} \right). \quad (2.33)$$

where due to the incompressibility condition $\nabla \cdot \mathbf{v}_t = \Gamma_t/\phi_n$. Therefore, one has

$$\dot{\mathbf{T}}'_t + \frac{\mu_t}{\eta_p} \left[1 - \frac{\phi_n\tau}{f(\mathbf{T}'_t)} \right]_+ \mathbf{T}'_t = 2\mu_t \left(\phi_n\mathbf{D}_t - \frac{\Gamma_t}{3}\mathbf{I} \right). \quad (2.34)$$

In absence of plastic deformation, i.e., for $f(\mathbf{T}'_t) < \phi_n\tau$, (2.34) reduces to the constitutive model proposed in [4, 5, 6, 29] (with $E = 3\mu_t\phi_n$ and dropping the convective derivatives).

On the other hand, we observe that in (2.34), the term containing the yield stress plays the role of a stress relaxation term that switches on only when the stress is above the yield value.

Referring to classical viscoelasticity [22, 28], the ratio η_p/μ_t identifies the characteristic time needed to relax the stress to the yield value (not to zero as for Maxwell fluids) and will be called here *plastic rearrangement time*. The limit $\eta_p \gg \mu_t$ leads once again to [4, 5, 6, 29]. However, in this case the procedure is incompatible with the small deformation assumption because the stress relaxes very slowly and so large stresses and deformation can build up.

On the other hand, rewriting (2.34) as

$$\frac{\eta_p}{\mu_t} \dot{\mathbf{T}}'_t + \left[1 - \frac{\phi_n\tau}{f(\mathbf{T}'_t)} \right]_+ \mathbf{T}'_t = 2\eta_p \left(\phi_n\mathbf{D}_t - \frac{\Gamma_t}{3}\mathbf{I} \right). \quad (2.35)$$

it is easy to realize that the limit $\eta_p \ll \mu_t$ with τ tending to zero leads to the viscous limit with viscosity η_p that can be found in [19, 20, 21] as a constitutive model for a constrained mixture. Following the same argument proposed in [37] one can state that in transient phenomena for times much larger than *plastic rearrangement time* the natural configuration has evolved relaxing the stress, leaving the material in a state of stress living on the yield surface.

3 One-Dimensional Problems

The equations of motion simplify considerably in the case of one-dimensional motion. The most important simplification is that the deformation tensor can be described by a scalar that relates Eulerian and Lagrangian coordinates through the volume ratio. The second simplification is that in one dimension a divergence-free velocity field is constant.

In fact, in one-dimensional problems one has the following system of equations

$$\left\{ \begin{array}{l} \frac{\partial\phi_0}{\partial t} + \frac{\partial}{\partial z}(\phi_0 v_0) = 0, \\ \frac{\partial\phi_t}{\partial t} + \frac{\partial}{\partial z}(\phi_t v_t) = \Gamma_t, \\ \frac{\partial}{\partial z}(\phi_0 v_0 + \phi_t v_t + \phi_\ell v_\ell) = 0, \\ v_\ell - v_t = -\frac{K}{\phi_\ell} \frac{\partial P}{\partial z}, \\ v_0 - v_t = \frac{K_0}{\phi_0^2} \left(-\phi_0 \frac{\partial P}{\partial z} + \frac{\partial T_0}{\partial z} \right), \\ -\frac{\partial P}{\partial z} + \frac{\partial}{\partial z}(T_0 + T_t) = 0, \end{array} \right. \quad (3.1)$$

where to simplify the notation we denoted by T_0 and T_t the stresses $T_{0,zz}$ and $T_{t,zz}$, respectively.

Exploiting a symmetry argument the third equation in (3.1) implies that $\phi_0 v_0 + \phi_t v_t + \phi_\ell v_\ell = 0$, which together with the last three equations determines

$$\begin{aligned} v_0 &= \left(K + \frac{(1-\phi_0)^2}{\phi_0^2} K_0 \right) \frac{\partial T_0}{\partial z} + \left(K - \frac{1-\phi_0}{\phi_0} K_0 \right) \frac{\partial T_t}{\partial z}, \\ v_\ell &= \left(-\frac{\phi_t + \phi_0}{1-\phi_t-\phi_0} K - \frac{1-\phi_0}{\phi_0} K_0 \right) \frac{\partial T_0}{\partial z} + \left(-\frac{\phi_t + \phi_0}{1-\phi_t-\phi_0} K + K_0 \right) \frac{\partial T_t}{\partial z}, \\ v_t &= \left(K - \frac{1-\phi_0}{\phi_0} K_0 \right) \frac{\partial T_0}{\partial z} + (K + K_0) \frac{\partial T_t}{\partial z}. \end{aligned} \quad (3.2)$$

In particular, combining the mass balance equations with the form assumed by the velocities one can write

$$\begin{cases} \frac{\partial \phi_0}{\partial t} + \frac{\partial}{\partial z} \left[\left(\phi_0 K + \frac{(1-\phi_0)^2}{\phi_0} K_0 \right) \frac{\partial T_0}{\partial z} + \phi_0 (K + K_0) \frac{\partial T_t}{\partial z} \right] = 0, \\ \frac{\partial \phi_t}{\partial t} + \frac{\partial}{\partial z} \left[\phi_t \left(K + \frac{1-\phi_0}{\phi_0} K_0 \right) \frac{\partial T_0}{\partial z} + (K + K_0) \frac{\partial T_t}{\partial z} \right] = \Gamma_t. \end{cases} \quad (3.3)$$

Notice that if the ECM is very soft, i.e. $T_0 \ll T_t$, then

$$\begin{aligned} v_t &\approx (K + K_0) \frac{\partial T_t}{\partial z}, \\ v_0 &\approx v_t - \frac{K_0}{\phi_0} \frac{\partial T_t}{\partial z}. \end{aligned}$$

On the other extreme, if the ECM is rigid ($v_0 = 0$) then

$$v_t = \frac{K K_0}{K \phi_0^2 + K_0 (1-\phi_0)^2} \frac{\partial T_t}{\partial z},$$

which implies that there is no motion if either K or K_0 goes to zero. In the former case, in fact the space is occupied by fibers. In the latter, adhesion with the fibers is quite strong. If $\phi_0 \rightarrow 0$, then $v_t = K \partial T_t / \partial z$, which is the type of relation used for instance in [16].

3.1 Homogeneous Growth of a Tumor in a Cylindrical Duct

To be more specific consider the case in which the tumor homogeneously grows inside a rigid cylinder. This situation resembles, for instance, the growth of a ductal carcinoma. Since the cylinder walls are supposed to be rigid, we assume deformations and velocities of all constituents to be along the duct axis z . Focusing on the extracellular matrix one then has

$$\mathbf{F}_0 = \text{Diag} \{1, 1, J_0\}, \quad \mathbf{B}_0 = \text{Diag} \{1, 1, J_0^2\}, \quad \text{with } J_0 = \frac{\bar{\phi}_0}{\phi_0}, \quad (3.4)$$

where $\text{Diag}\{\cdot\}$ stands for a diagonal matrix. Similarly for the tumor

$$\mathbf{F}_t = \text{Diag} \{1, 1, \Lambda_t\}, \quad \mathbf{F}_n = \text{Diag} \{\lambda_n, \lambda_n, \Lambda_n\}, \quad \mathbf{F}_p = \text{Diag} \{\lambda_p, \lambda_p, \Lambda_p\}, \quad (3.5)$$

and

$$\mathbf{B}_n = \text{Diag} \{\lambda_n^2, \lambda_n^2, \Lambda_n^2\}, \quad \mathbf{D}_p = \text{Diag} \{\dot{\lambda}_p \lambda_p^{-1}, \dot{\lambda}_p \lambda_p^{-1}, \dot{\Lambda}_p \Lambda_p^{-1}\}. \quad (3.6)$$

Equations (1.1), (1.3c), and (1.3d) imply that

$$\begin{cases} F_{t,rr} = 1 = \lambda_n \lambda_p g, \\ F_{t,zz} = \Lambda_t = \Lambda_n \Lambda_p g, \\ \det(\mathbf{F}_p) = 1 = \lambda_p^2 \Lambda_p, \\ \det(\mathbf{F}_n) = \frac{\phi_n}{\phi_t} = \lambda_n^2 \Lambda_n, \end{cases} \quad (3.7)$$

that can be solved to give

$$\Lambda_t = \frac{\phi_n}{\phi_t} g^3, \quad \lambda_n = \frac{\sqrt{\Lambda_p}}{g}, \quad \Lambda_n = \frac{\phi_n g^2}{\phi_t \Lambda_p}, \quad \lambda_p = \frac{1}{\sqrt{\Lambda_p}}. \quad (3.8)$$

We explicitly remark that given Λ_p and g , B_{zz} is given by

$$B_{zz} = \frac{\phi_n^2}{\phi_t^2} \frac{g^4}{\Lambda_p^2}.$$

It is instructive to examine the case $B_{zz} = 1$, corresponding to no elastic deformations along the duct axis. For instance, if $\phi_t = \phi_n$ and the body is growing, Λ_p must be such that $\Lambda_p = g^2 > 1$ to achieve that, i.e., the body has to plastically rearrange and adapt in response to growth.

Now Bingham's constitutive equation for the evolution of \mathbf{F}_p gives

$$\dot{\lambda}_p = \dot{\Lambda}_p = 0, \quad \text{if } f\left(\mathbf{B}_n - \frac{1}{3}(\text{tr}\mathbf{B}_n)\mathbf{I}\right) \leq \frac{\tau}{\mu_t}, \quad (3.9)$$

where if we choose $f = f_2$ (see (2.16) applied to (2.17)), the yield condition reads

$$\frac{|\Lambda_n^2 - \lambda_n^2|}{2} \leq \tilde{\tau}, \quad (3.10)$$

where $\tilde{\tau} = \tau/\mu_t$ and

$$\begin{aligned} \dot{\lambda}_p &= \lambda_p \frac{\mu_t}{2\eta_p} \left[1 - \frac{\tau}{\mu_t f(\mathbf{B}_n - \frac{1}{3}(\text{tr}\mathbf{B}_n)\mathbf{I})} \right] \left(\lambda_n^2 - \frac{1}{3}(2\lambda_n^2 + \Lambda_n^2) \right) \\ &= \lambda_p \frac{\mu_t}{2\eta_p} \left[1 - \frac{\tilde{\tau}}{f(\mathbf{B}_n - \frac{1}{3}(\text{tr}\mathbf{B}_n)\mathbf{I})} \right] \frac{\lambda_n^2 - \Lambda_n^2}{3}, \end{aligned} \quad (3.11)$$

$$\begin{aligned} \dot{\Lambda}_p &= \Lambda_p \frac{\mu_t}{2\eta_p} \left[1 - \frac{\tau}{\mu_t f(\mathbf{B}_n - \frac{1}{3}(\text{tr}\mathbf{B}_n)\mathbf{I})} \right] \left(\Lambda_n^2 - \frac{1}{3}(2\lambda_n^2 + \Lambda_n^2) \right) \\ &= \Lambda_p \frac{\mu_t}{\eta_p} \left[1 - \frac{\tilde{\tau}}{f(\mathbf{B}_n - \frac{1}{3}(\text{tr}\mathbf{B}_n)\mathbf{I})} \right] \frac{\Lambda_n^2 - \lambda_n^2}{3}, \end{aligned} \quad (3.12)$$

otherwise.

It can be easily checked that Eq.(2.4) holds and

$$\begin{aligned} \dot{J}_p &= 2\lambda_p \dot{\lambda}_p \Lambda_p + \lambda_p^2 \dot{\Lambda}_p \\ &= 2\lambda_p^2 \Lambda_p \frac{\mu_t}{2\eta_p} \left[1 - \frac{\tilde{\tau}}{f(\mathbf{B}_n)} \right] \frac{\lambda_n^2 - \Lambda_n^2}{3} + \lambda_p^2 \Lambda_p \frac{\mu_t}{\eta_p} \left[1 - \frac{\tilde{\tau}}{f(\mathbf{B}_n)} \right] \frac{\Lambda_n^2 - \lambda_n^2}{3} = 0. \end{aligned} \quad (3.13)$$

Using Eq.(3.8), (3.9)–(3.12) can be summarized in

$$\dot{\Lambda}_p = \frac{\mu_t}{3\eta_p} \left[1 - \frac{\tilde{\tau}}{f(\mathbf{B}_n)} \right]_+ \left(\frac{\phi_n^2}{\phi_t^2} \frac{g^4}{\Lambda_p} - \frac{\Lambda_p^2}{g^2} \right), \quad (3.14)$$

where

$$f(\mathbf{B}_n) = \frac{1}{2} \left(\frac{\phi_n^2}{\phi_t^2} \frac{g^4}{\Lambda_p^2} - \frac{\Lambda_p}{g^2} \right). \quad (3.15)$$

In particular, the yield condition (3.10) is given by

$$\frac{1}{2} \left| \frac{\phi_n^2}{\phi_t^2} \frac{g^4}{\Lambda_p^2} - \frac{\Lambda_p}{g^2} \right| \leq \tilde{\tau}. \quad (3.16)$$

For sake of completeness we recall that

$$\lambda_p = -\frac{\mu_t}{6\eta_p} \left[1 - \frac{\tilde{\tau}}{f(\mathbf{B}_n)} \right]_+ \left(\frac{\phi_n^2}{\phi_t^2} g^4 \lambda_p^5 - \frac{1}{g^2 \lambda_p} \right), \quad (3.17)$$

and $\lambda_p^2 \Lambda_p = 1$.

The last equation to take into account to describe the evolution of the natural configuration is (1.10).

In conclusion, one can then simplify the system (3.1) in

$$\begin{cases} \frac{\partial \phi_0}{\partial t} + \frac{\partial}{\partial z}(\phi_0 v_0) = 0, \\ \frac{\partial \phi_t}{\partial t} + \frac{\partial}{\partial z}(\phi_t v_t) = \Gamma_t, \\ \frac{\partial g}{\partial t} + v_t \frac{\partial g}{\partial z} = \frac{\Gamma_t}{3\phi_t} g, \\ \frac{\partial \Lambda_p}{\partial t} + v_t \frac{\partial \Lambda_p}{\partial z} = \frac{\mu_t}{3\eta_p} \left[1 - \frac{\tilde{\tau}}{f(\mathbf{B}_n)} \right]_+ \left(\frac{\phi_n^2}{\phi_t^2} \frac{g^4}{\Lambda_p} - \frac{\Lambda_p}{g^2} \right), \end{cases} \quad (3.18)$$

with

$$\begin{cases} v_0 = \left(K + \frac{(1-\phi_0)^2}{\phi_0^2} K_0 \right) \frac{\partial T_0}{\partial z} + \left(K - \frac{1-\phi_0}{\phi_0} K_0 \right) \frac{\partial T_t}{\partial z}, \\ v_t = \left(K - \frac{1-\phi_0}{\phi_0} K_0 \right) \frac{\partial T_0}{\partial z} + (K + K_0) \frac{\partial T_t}{\partial z}, \\ T_0 = \phi_0 \left(-\Sigma_0 \left(\frac{\bar{\phi}_0}{\phi_0} \right) + \mu_0 \frac{\bar{\phi}_0^2}{\phi_0^2} \right), \\ T_t = \phi_t \left(-\Sigma_t \left(\frac{\phi_n}{\phi_t} \right) + \mu_t \frac{\phi_n^2}{\phi_t^2} \frac{g^4}{\Lambda_p^2} \right). \end{cases} \quad (3.19)$$

In addition,

$$T_{t,rr} = \mu_t \phi_t \left(-\Sigma_t + \frac{\Lambda_p}{g^2} \right).$$

With simple modifications the same procedure illustrated above applies to the axisymmetric growth of a tumor cord around a capillary and to the spherical growth of a multicellular spheroid.

Remark. Plasticity implies that \mathbf{T}_t stays on the yield surface; in one-dimensional problems this condition translates into the following relationship between the strains

$$2f \left(\frac{\phi_n}{\phi_t} \frac{g^2}{\Lambda_p}, \frac{\sqrt{\Lambda_p}}{g} \right) = \tilde{\tau},$$

replacing the evolution equation for Λ_p . For instance, in the case $f = f_2$, Λ_p is such that

$$\frac{1}{2} \left| \frac{\phi_n^2 g^4}{\phi_t^2 \Lambda_p^2} - \frac{\Lambda_p}{g^2} \right| = \tilde{\tau}.$$

From the condition above one can then compute Λ_p in terms of g , i.e. the plastic deformation in terms of growth to remain on the yield surface.

This limit is obtained in the last equation in (3.18) for very small plastic rearrangement times, i.e., $\eta_p/\mu_t \ll 1$.

4 Numerical simulations

In the simulation to follow we use a growth term similar to the one used in [16] to take contact inhibition of growth into account while neglecting the effect of nutrients and other growth factors. We will then assume that cells replicate only if the local volume ratio (or stress) is below a threshold value, otherwise they become quiescent. In addition a physiological death term is introduced so that the growth term can be modelled as

$$\Gamma_T = [\gamma H_\sigma(\bar{\phi} - \phi_T) - \delta] \phi_T \quad (4.20)$$

where H_σ is a regularization of the Heaviside function of width σ vanishing for $\phi_t > \bar{\phi}$, so that $\bar{\phi}$ is the limit value allowing proliferation. The value of $\bar{\phi}$ referring to the tumor is slightly larger than that referring to the normal tissue. The stress functions Σ_0 and Σ_t are modelled in the following simplest way

$$\Sigma_0 = \mu_0 \frac{\phi_0}{\bar{\phi}_0}, \quad \Sigma_t = \mu_t \frac{\phi_t}{\phi_n}. \quad (4.21)$$

The equations are rewritten in non-dimensional form: scaling time with $1/\gamma$ and lengths with $\sqrt{\frac{K\mu_t}{\gamma}}$. Considering that the elastic modulus of a soft tissue like a mammary gland is of the order of 100 Pa [36], that the permeability K is of the order of $10^{-13} \text{ m}^2/(\text{Pa s})$ [34] and that the growth rate is of the order of one day [30, 15] then the typical time is of the order of one day and the typical length is of the order of one millimeter. We recall that ϕ_0 , ϕ_t , g , and Λ_p are already dimensionless.

The following dimensionless numbers characterize the evolution equations

- $\tilde{K} = K_0/K$, is the ratio between the interaction force between tumor cells and the liquid flowing around it and the one between tumor cells and the ECM. It is then expected to be one or two orders of magnitude smaller than one.
- $\tilde{\mu} = \mu_0/\mu_t$, which refer to the ratio between the elastic moduli of the ECM and that of the ensemble of tumor cells.
- $\tilde{\tau} = \tau/\mu_t$, is the ratio between the yield stress and the Young modulus. Since the former seems to be of the order of 1 Pa (or at most 100 Pa), this number is smaller than one.
- $\tilde{\eta}_p = \nu\eta_p/\mu_t$, is the ratio between the characteristic stress relaxation time due to cell reorganization and the duplication time. Since the former is of the order of minutes up to few hours, it is at least an order of magnitude smaller than the characteristic time chosen on the basis of the duplication time.
- $\tilde{\delta} = \delta/\gamma$, is the ratio between the apoptotic and the growth rate.

Equation (3.18) remain formally unchanged if space, time and velocities are considered dimensionless and μ_t/η_p is replaced by $1/\tilde{\eta}_p$. We instead specialise Eq. (3.19) for sake of completeness

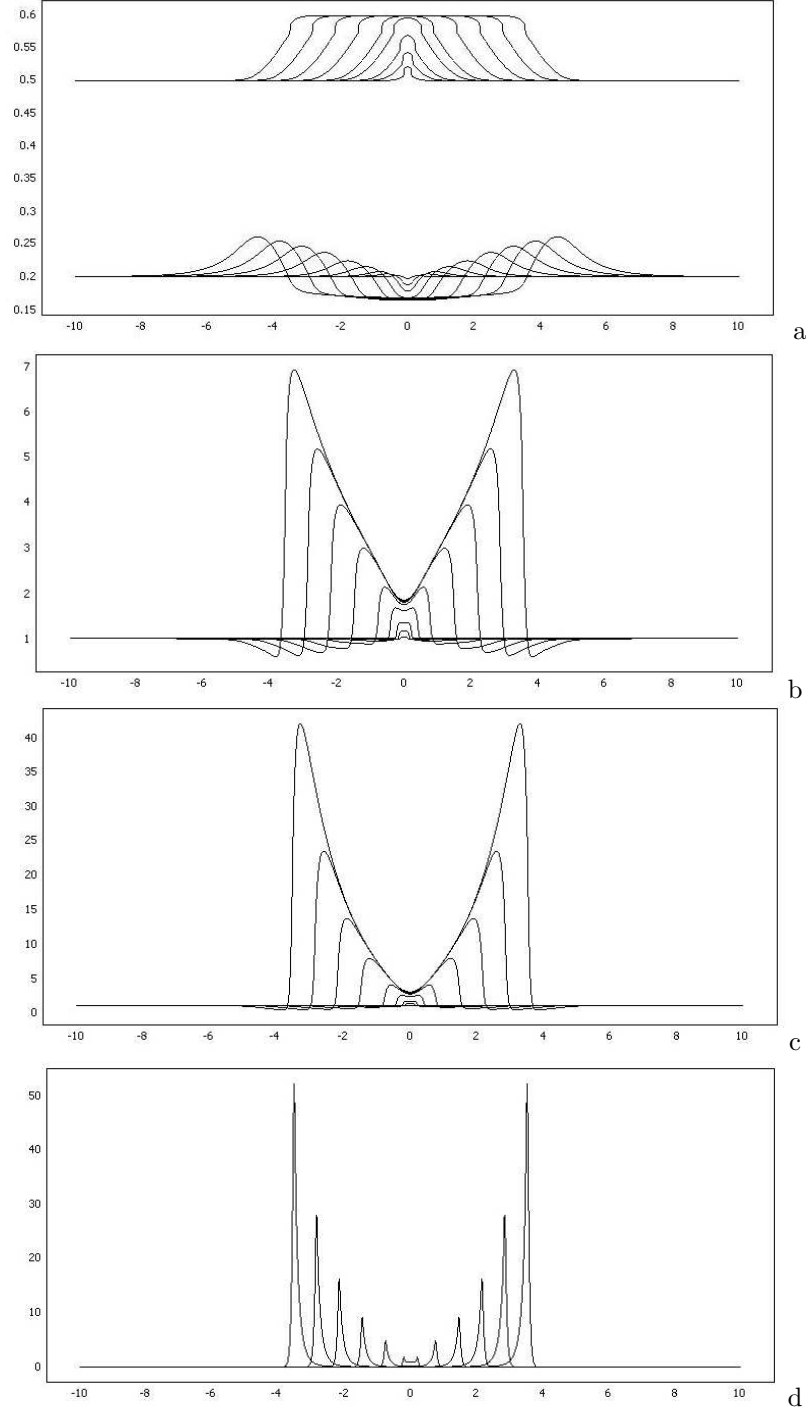


Figure 3: Tumor growth in a tissue for $\tilde{K} = 0.1$, $\tilde{\mu} = 0.1$, $\tilde{\tau} = 0.01$, $\tilde{\eta}_p = 0.01$, and $\tilde{\delta} = 0.1$ at $\tilde{t} = 0.1, 0.5, 1, 2, 4, 8, 12, 16, 20$. (a) Cell volume ratio (upper set of curves) and ECM volume ratio (lower set of curves) versus space. The region occupied by the tumor is the central region. Its borders can be well identified by the inflection points (points with almost vertical slopes). The outer region is occupied by the host tissue. (b) Growth. (c) Plastic deformation. (d) $\dot{\Lambda}_p$ (only for $\tilde{t} = 0.1, 1, 4, 8, 12, 16, 20$ for sake of clarity).

(dropping tildas for the velocities and the stresses)

$$\left\{ \begin{array}{l} v_0 = \left(1 + \frac{(1 - \phi_0)^2 \tilde{K}}{\phi_0^2} \right) \frac{\partial T_0}{\partial z} + \left(1 - \frac{1 - \phi_0 \tilde{K}}{\phi_0} \right) \frac{\partial T_t}{\partial z}, \\ v_t = \left(1 - \frac{1 - \phi_0 \tilde{K}}{\phi_0} \right) \frac{\partial T_0}{\partial z} + \left(1 + \tilde{K} \right) \frac{\partial T_t}{\partial z}, \\ T_0 = -\tilde{\mu} \phi_0 \left(\frac{\phi_0}{\bar{\phi}_0} - \frac{\bar{\phi}_0^2}{\phi_0^2} \right), \\ T_t = -\phi_t \left(\frac{\phi_t}{\phi_n} - \frac{\phi_n^2}{\phi_t^2} \frac{g^4}{\Lambda_p^2} \right). \end{array} \right. \quad (4.22)$$

The values used in the following simulations are given in Table 1.

Parameter	Estimated value
$\tilde{\delta}$	0.1
$\bar{\phi}$	0.5
ϕ_n	0.49
$\bar{\phi}_0$	0.2
K	0.01–0.1
$\tilde{\mu}$	0.01–0.1
$\tilde{\tau}$	0.01–0.1
$\tilde{\eta}_p$	0.01–0.1

Table 1: Parameters.

Initially a tumor is located in the interval $x \in [-0.1, 0.1]$. The initial volume ratio is equal to 0.5 everywhere. Similarly to what done in [16] tumor cells are assumed to be less sensitive to compression and to stop duplicating only when the volume ratio reaches $\bar{\phi} = 0.6$.

The general feature of the simulation is the following: initially the ensemble of tumor cells starts growing and compressing the tissue outside. Upon reaching the value of contact inhibition of the tumor, cells stop duplicating in the core of the tumor and continue duplicating close to the border, compressing more and more the tissue outside. When the compression of the surrounding tissue gets larger than that allowing duplication cells die without reproduction. At the same time, the ECM is dragged by the expanding motion of the tumor cells forming a sort of capsule at the border of the tumor.

Specifically, Figure 3a shows the volume ratio quickly increasing in the center of the tumor ($x = 0$) from the rest value for a normal tissue to the one in which also tumor cell duplication is controlled by contact inhibition. This is also evident in Figure 3b where the growth function increases from the initial unitary value, causing a corresponding increase in Λ_p (Figure 3c). About $\tilde{t} = 2$, the growth function g reaches in the center a stationary value, corresponding to no net growth. This brings to no evolution in the natural configuration in the central region and Λ_p and ϕ_t tending to a stationary value. The region where there is evolution of the natural configuration due to plastic deformation is shown in Figure 3d. Far from the central region, the interface dividing the tumor from the surrounding tissue can be identified in Figure 3a by the strong variation in volume ratio. After $\tilde{t} > 2$ the maximum growth (due to contact inhibition in the core of the tumor) and the maximum plastic deformations occur at the tumor boundary (see Figures 3b,c,d). Outside the tumor region the host tissue is compressed to a value high enough that host cells start dying, as can be deduced from Figure 3b where $g < 1$ implies tissue resorption, also implying $\Lambda_p < 1$ (Figure 3c). Considering the time evolution of the volume ratio, it appears that for longer times ϕ_t exhibits the profile of a travelling wave, while the components leading to the evolution

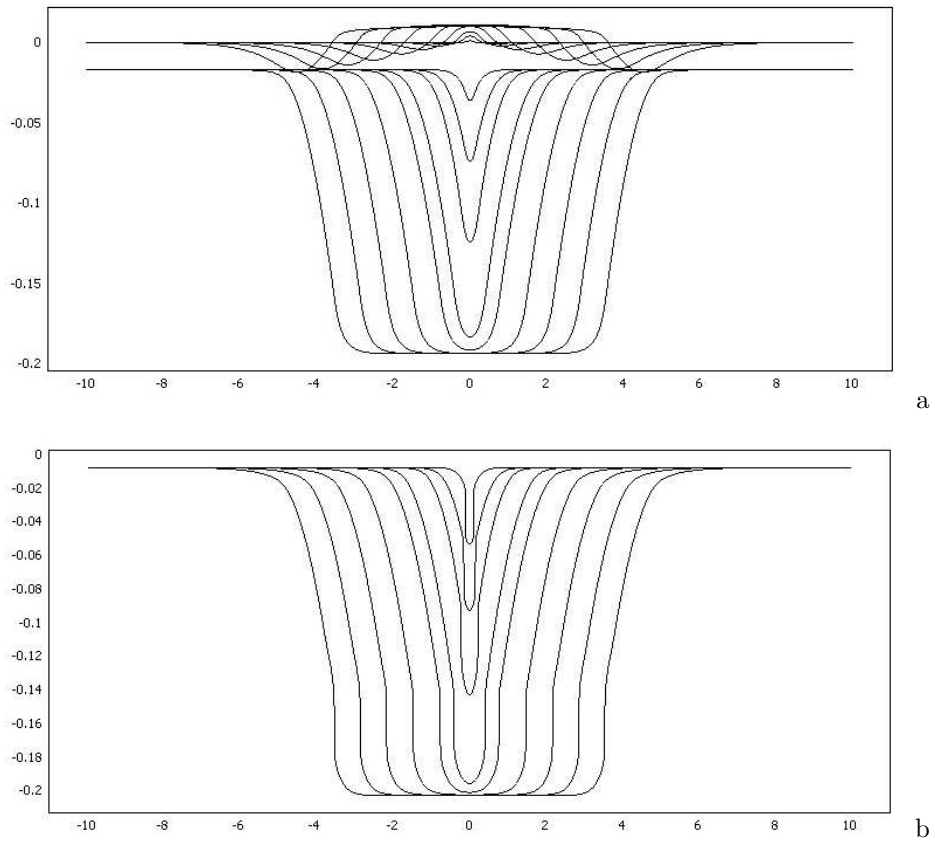


Figure 4: Stress evolution in a growing tumor for for the same times and parameters as in Figure 3. (a) Axial stress related to the tumor constituent (lower set of curves) and ECM (upper set of curves) (b) Radial stress acting on the duct wall.

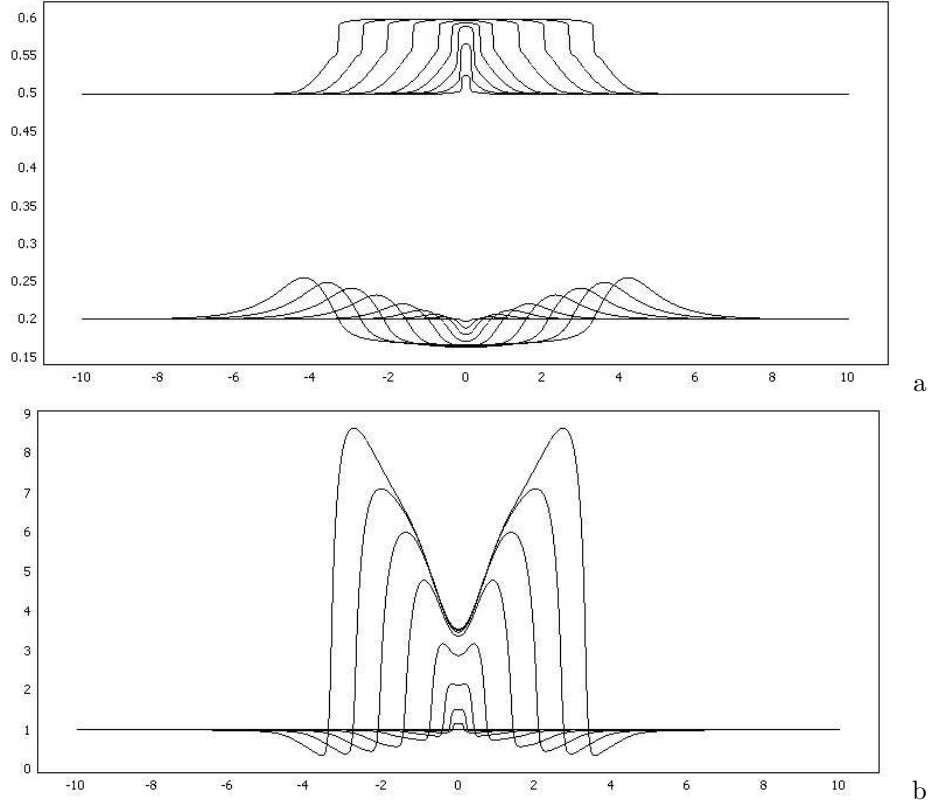


Figure 5: Tumor growth in a tissue for the same times and parameters as in Figure 3, but $\tilde{\eta}_p$ that increases to 0.1. (a) Cell volume ratio (upper set of curves) and ECM volume ratio (lower set of curves). (b) Plastic deformation.

of the natural configurations continue to increase with time. At the same time, the extra-cellular matrix is dragged by the tumor expansion, thus forming a sort of capsule at the border of the tumor (minimum of ECM volume ratio in the center of the tumor and maximum in the host tissue close to the boundary). No mechanisms of ECM degradation and remodelling is included in the model, so that the mass of ECM is preserved and simply displaced. We observe that, as might be expected, the stiffer the ECM is (i.e., larger $\tilde{\mu}$), the smaller the accumulation of ECM is at the border of the tumor (results not shown).

The time evolution of the stresses is given in Figure 4. Considering the axial components of the partial stresses represented in Figure 4a, the one referring to the tumor constituents is in compression, while the ECM is in tension inside the tumor and in compression outside it, due to the formation of the capsule, i.e. the region with higher concentration of ECM. Figure 4b instead refers to the stress that a growing tumor exerts on the duct wall.

The role of the parameters related to the description of the elasto-viscoplastic behaviors of tumors, namely $\tilde{\tau}$ and $\tilde{\eta}_p$ is detailed in Figures 5 and 6. In Figure 5 $\tilde{\eta}_p$ increases to 0.1 i.e., in dimensional terms, the plastic reorganization time increases from several minutes to a few hours. As shown in Figure 5a, the evolution of cell and ECM concentration does not vary significantly: the time needed to reach in the tumor center the growth inhibitory concentration halves, growth is a bit slower, and the “jump” near the tumor-host interface is stronger. Figure 5b shows that in the center growth and plastic deformation and therefore the evolution of the natural configuration takes longer to reach the stationary value.

A stronger difference is found increasing the yield stress $\tilde{\tau}$ to 0.1, corresponding to stronger

adhesive bonds among cells. The increase in yield stress keeps the tumor more compact, which gives rise to a decrease in growth rates (see Figure 6b,c,d). The final result is a stronger decrease in the expansion velocity, which more or less halves. Deformation of the ECM is much smaller, without the formation of a capsule around the tumor (see Figure 6a).

Final Remarks

The mathematical model of a solid tumor illustrated in the present paper collects a number of features that have been pointed out in the recent literature: three-dimensional formulation, use of mixture theory, stress-growth relationships, cell adhesion. Apart from the interest in a unified presentation of these aspects, the novelty of the present formulation is in its capability to account for the mechanical behavior of a conglomeration of cells that are weakly bounded to each other.

In fact, a fully elastic model can yield to large unrealistic tensions in the tumor (as pointed out, for instance, by Volokh [45]), while viscous fluid models do not account for simple phenomenological arguments. The introduction of an elasto-viscoplastic constitutive law provides a mechanism for stress relaxation while preserving a precise mathematical framework to the theory. Previously proposed constitutive models are obtained as limit cases. Experiments in this direction will supply measures of yield stress and will possibly clarify under what conditions simpler models are acceptable. In this respect, in addition to uni-axial tests like those performed in [8, 14, 35, 44] it would be very important to perform shear tests on multicellular spheroids, also interfering with the adhesion molecules by modifying the anchorage mechanism, or by the use of antibodies of the extracellular domain.

From the modelling viewpoint, the model proposed here can be developed further by treating in more detail the adhesion mechanisms between cells and the different constituents of the extracellular matrix. In fact, both the adhesion mechanisms involving cadherins and integrins are relevant to understand tissue invasion by the tumor. Other developments can be obtained taking into account of ECM remodelling through the production of matrix degrading enzymes and of the influence of nutrients and chemical factors, such as growth promoting factors and growth inhibitory factors, both diffusible and bounded to the ECM.

Acknowledgements

Partially supported by the European Community, through the Marie Curie Research Training Network Project HPRN-CT-2004-503661: Modelling, Mathematical Methods and Computer Simulation of Tumor Growth and Therapy and by the Italian Ministry for University and Research, through a PRIN project on Modelli matematici di crescita e vascolarizzazione di tumori e tessuti biologici.

References

- [1] D. Ambrosi and F. Mollica (2002). On the mechanics of a growing tumor, *Int. J. Engng. Sci.* **40**: 1297–1316.
- [2] D. Ambrosi and F. Mollica (2004). The role of stress in the growth of a multicell spheroid, *J. Math. Biol.* **48**: 477–499.
- [3] D. Ambrosi and L. Preziosi (2002). On the closure of mass balance models for tumor growth, *Math. Mod. Meth. Appl. Sci.* **12**: 737–754.
- [4] R.P. Araujo and D.L.S. McElwain (2005). A mixture theory for the genesis of residual stresses in growing tissues, I: A general formulation, *SIAM J. Appl. Math.* **65**: 1261–1284.

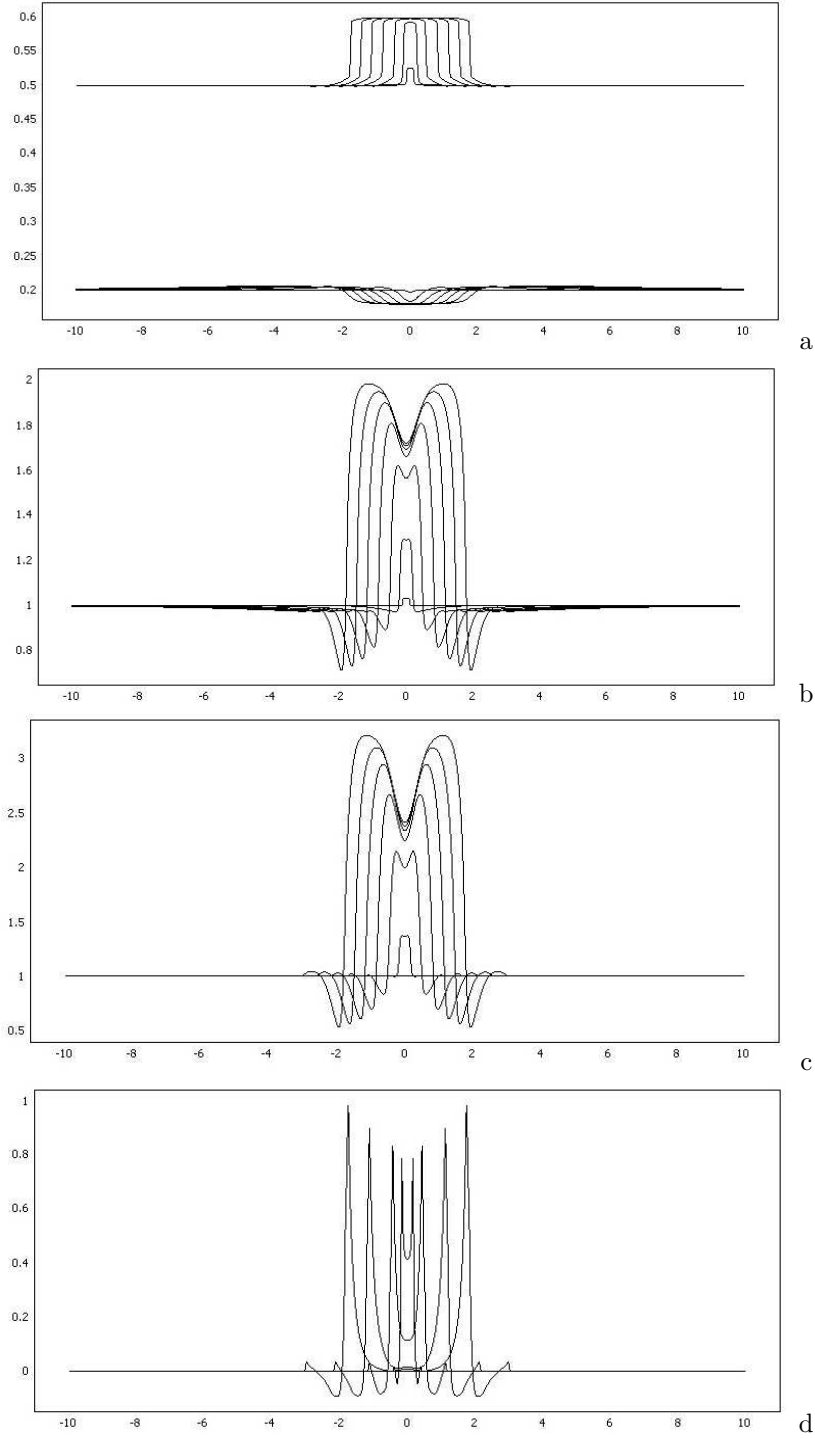


Figure 6: Tumor growth in a tissue for the same parameters as in Figure 3, but $\tilde{\tau}$ that increases to 0.1 at $\tilde{t} = 0.1, 1, 4, 8, 12, 16, 20$. (a) Cell volume ratio (upper set of curves) and ECM volume ratio (lower set of curves). The region occupied by the tumor is the central region. Its borders can be well identified by the inflection points (points with almost vertical slopes). The outer region is occupied by the normal tissue. (b) Growth. (c) Plastic deformation. (d) $\dot{\Lambda}_p$ (only for $\tilde{t} = 0.1, 1, 4, 12, 20$ for sake of clarity).

- [5] R.P. Araujo and D.L.S. McElwain (2005). A mixture theory for the genesis of residual stresses in growing tissues, II: Solutions to the biphasic equations for a multicell spheroid, *SIAM J. Appl. Math.* **65**: 1285–1299.
- [6] R.P. Araujo and D.L.S. McElwain (2004). A linear-elastic model of anisotropic tumour growth, *Eur. J. Appl. Math.* **15**: 365–384.
- [7] I.V. Basov and V.V. Shelukhin (1999). Generalized solutions to the equations of compressible Bingham flows, *Z. Angew. Math. Mech.* **79**: 185–192.
- [8] W. Baumgartner, P. Hinterdorfer, W. Ness, A. Raab, D. Vestweber, H. Schindler, and D. Drenkhahn (2000). Cadherin interaction probed by atomic force microscopy, *Proc. Nat. Acad. Sci. USA* **97**: 4005–4010.
- [9] C.J.W. Breward, H.M. Byrne, and C.E. Lewis (2002). The role of cell-cell interactions in a two-phase model for avascular tumor growth, *J. Math. Biol.* **45**: 125–152.
- [10] C.J.W. Breward, H.M. Byrne, and C.E. Lewis (2003). A multiphase model describing vascular tumor growth, *Bull. Math. Biol.* **65**: 609–640.
- [11] R. Buscall, P.D.A. Mills, J.W. Goodwin, and D.W. Lawson (1988). Scaling behaviour of the rheology of aggregate networks formed from colloidal particles, *J. Chem. Soc. Faraday Trans.* **84**: 4249–4260.
- [12] H.M. Byrne, J.R. King, D.L.S. McElwain, and L. Preziosi, (2003). A two-phase model of solid tumor growth, *Appl. Math. Letters* **16**: 567–573.
- [13] H.M. Byrne and L. Preziosi (2004). Modeling solid tumor growth using the theory of mixtures, *Math. Med. Biol.* **20**: 341–366.
- [14] E. Canetta, A. Duperray, A. Leyrat and C. Verdier, (2005). Measuring cell viscoelastic properties using a force-spectrometer: Influence of the protein-cytoplasm interactions, *Biorheology* **42**: 298–303.
- [15] L. Caveda, I. Martin-Padura, P. Navarro, F. Breviario, M. Corada, D. Gulino, M.G. Lampugnani, and E. Dejana (1996). Inhibition of cultured cell growth by vascular endothelial cadherin (cadherin-5/VE-cadherin), *J. Clin. Invest.* **98**: 886–893.
- [16] M. Chaplain, L. Graziano, and L. Preziosi (2006). Mathematical modelling of the loss of tissue compression responsiveness and its role in solid tumour development, *Math. Med. Biol.* **23**: 197–229.
- [17] C.Y. Chen, H.M. Byrne and J.R. King (2001), The influence of growth-induced stress from the surrounding medium on the development of multicell spheroids, *J. Math. Biol.* **43**: 191–220.
- [18] G. Forgacs, R.A. Foty, Y. Shafrir, and M.S. Steinberg (1998), Viscoelastic properties of living embryonic tissues: a quantitative study, *Biophys. J.* **74**: 2227–2234.
- [19] S.J. Franks, H.M. Byrne, J.R. King, J.C.E. Underwood, and C.E. Lewis (2003). Modelling the early growth of ductal carcinoma in situ of the breast, *J. Math. Biol.* **47**: 424–452.
- [20] S.J. Franks, H.M. Byrne, H.S. Mudhar, J.C.E. Underwood, and C.E. Lewis (2003). Mathematical modelling of comedo ductal carcinoma in situ of the breast, *Math. Med. Biol.* **20**: 277–308.
- [21] S.J. Franks and J.R. King (2003). Interactions between a uniformly proliferating tumor and its surrounding. Uniform material properties, *Math. Med. Biol.* **20**: 47–89.
- [22] R.F. Gibson (1994). **Principles of Composite Material Mechanics**, McGraw-Hill.

- [23] A.E. Green and P.M. Naghdi (1969), On basic equations for mixtures, *Quart. J. Mech. Appl. Math.*, **22**:4, 427-438.
- [24] G. Helmlinger, P.A. Netti, H.C. Lichtenbeld, R.J. Melder, and R.K. Jain (1997). Solid stress inhibits the growth of multicellular tumour spheroids, *Nature Biotech.* **15**: 778–783.
- [25] K. Hohenemser and W. Prager (1932). Über die ansätze der mechanik isotroper kontinua, *ZAMM* **12**: 216–226.
- [26] J.D. Humphrey and K.R. Rajagopal (2002). A constrained mixture model for growth and remodeling of soft tissues, *Math. Mod. Meth. Appl. Sci.* **12**: 407–430.
- [27] J.D. Humphrey and K.R. Rajagopal (2003). A constrained mixture model for arterial adaptations to a sustained step-change in blood flow, *Biomech. and Model. Mechanobiol.* **2**: 109–126.
- [28] D.D. Joseph (1990). **Fluid Dynamics of Viscoelastic Liquids**, Springer.
- [29] A.F. Jones, H.M. Byrne, J.S. Gibson, and J.W. Dold (2000). A mathematical model of the stress induced during solid tumour growth, *J. Math. Biol.* **40**: 473–499.
- [30] S. Levenberg, A. Yarden, Z. Kam, and B. Geiger (1999). p27 is involved in N-cadherin-mediated contact inhibition of cell growth and S-phase entry, *Oncogene* **18**: 869–876.
- [31] L.E. Malvern (1969). **Introduction of the Mechanics of a Continuous Medium**, Prentice Hall Inc.
- [32] S.M. Klisch and A. Hoger (2003). Volumetric growth of thermoelastic materials and mixtures, *Math. Mech. Solids* **8**: 377–402.
- [33] F. Mollica, L. Preziosi, K.R. Rajagopal (2007). **Modelling of Biological Materials**, Birkhäuser.
- [34] P.A. Netti and R.K. Jain (2003). Interstitial transport in solid tumours, in **Cancer Modelling and Simulation**, L. Preziosi, Ed., CRC-Press - Chapman Hall, Boca Raton.
- [35] P. Panorchan, M.S. Thompson, K.J. Davis, Y. Tseng, K. Konstantopoulos, and D. Wirtz (2006). “Single-molecule analysis of cadherin-mediated cell-cell adhesion”, *J. Cell Sci.* **119**: 66–74.
- [36] M.J. Paszek, N. Zahir, K.R. Johnson, J.N. Lakins, G.I. Rozenberg, A. Gefen, C.A. Reinhart-King, S.S. Margulies, M. Dembo, D. Boettiger, D.A. Hammer, and V. M. Weaver (2005) Tensional homeostasis and the malignant phenotype, *Cancer Cell* **8**: 241–254.
- [37] L. Preziosi and D. D. Joseph (1987). Stokes’ first problem for viscoelastic fluids, *J. Non-Newtonian Fluid Mech.*, **25**: 239–259.
- [38] L. Preziosi and A. Tosin (2007). “Multiphase modeling of tumor growth and extracellular matrix interaction: Mathematical tools and applications”, *J. Math. Biol.* in press.
- [39] I.J. Rao, J.D. Humphrey, and K.R. Rajagopal (2003). Biological growth and remodeling: A uniaxial example with possible application to tendons and ligaments, *Comp. Mod Engr. Sci.* **4**: 439–455.
- [40] T. Roose, P. A. Netti, L. L. Munn, Y. Boucher, R. K. Jain (2003) Solid stress generated by spheroid growth estimated using a linear poroelasticity model, *Microvascular Research*, **66**: 204–212.
- [41] T.W. Secomb and A.W. El-Kareh (2001). A theoretical model for the elastic properties of very soft tissues, *Biorheology* **38**: 305–317.

- [42] V.V. Shelukhin (2002). Bingham viscoplastic as a limit of non-Newtonian fluids, *J. Math. Fluid Mech.* **4**: 109–127.
- [43] P. Snabre and P. Mills (1996). Rheology of weakly flocculated suspensions of rigid particles, *J. Phys. III France* **6**: 1811–1834.
- [44] M. Sun, J.S. Graham, B. Hegedus, F. Marga, Y. Zhang, G. Forgacs, and M. Grandbois (2005). Multiple membrane tethers probed by atomic force microscopy, *Biophys. J.* **89**: 4320–4329.
- [45] K.Y. Volokh, (2006), Stresses in growing soft tissues, *Acta Biomater.* **2**: 493–504.
- [46] K. Wilmanski (1995), Lagrangean model of two-phase porous material. *J. Non-Equilibrium Thermodyn.* **20**: 50–77.